JOC*Article*

An Unusual Reaction of the Natural Compound Benaphthamycin B: Theoretical Study of a Model System†

Andreas Opitz,*,‡ Dong Wei-Opitz,‡ Peter Gebhardt,§ and Rainer Koch*,||

Fachbereich Chemie, Universität Konstanz, D-78457 Konstanz, Hans-Knöll-Institut für Naturstoff-Forschung, P.O. Box 100813, D-07708 Jena, and Institut für Reine und Angewandte Chemie, Carl von Ossietzky Universität Oldenburg, P.O. Box 2503, D-26111 Oldenburg, Germany

andreas.opitz@uni-konstanz.de; rainer.koch@uni-oldenburg.de

Received October 27, 2005

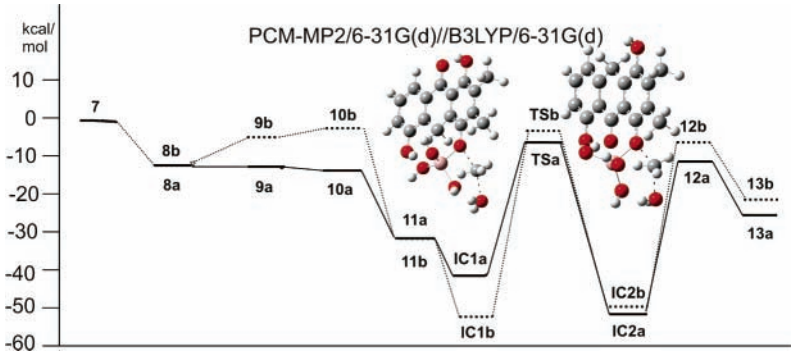

The surprising and complex transformation of benaphthamycin B to give quinone **2a** is investigated theoretically with a model compound, 1,5-dihydroxy-4-methoxy-2,3-dimethylanthraquinone (**3**). The detailed study is performed using both DFT and perturbation theory under inclusion of solvent effects. Several individual steps (reduction and hydrolysis, water elimination, ether cleavage, and oxidation) of the proposed reaction cascade calculated at the PCM-MP2/6-31G(d)//B3LYP/6-31G(d) level of theory are presented and discussed. It is shown that the key step, the ether cleavage as an S_N2 reaction leading to the anthrone **12a**, possesses a smaller activation barrier compared to the alternative process yielding **12b**. Therefore, the formation of the thermodynamically preferred model quinone **13a** is also the kinetically favored pathway: The results of the calculated model reaction should also be valid for benaphthamycin B (**1**).

Introduction

Natural compounds can be important as lead structures for pharmaceuticals.[1] Several naturally and also a few related nonnaturally occurring quinones, such as anthracyclines, e.g., daunorubicine, doxorubicine, idarubicine, and mithoxanthrone, attracted large interest because of their importance as anticancer agents.[2] Another important class of quinones with promising pharmaceutical activities are dihydrobenzo[*a*]naphthacenequinones, which are formed by *Streptomyces* sp. HKI-0057. One representative compound of this class is madura lactone and its open form, maduranic acid.[3] More than 250 derivatives of this compound, in particular, hydrazones, semicarbazones, and thiosemicarbazones, have been synthesized and tested.[3,4] Some of them show interesting activities against diverse targets, e.g., activity against Gram-positive bacteria, and gyrase inhibition. Further interesting derivatives are pradimicines[5] and benaphthamycin B (**1**).[4] During the synthesis of derivatives of **1** a complex and unusual reaction cascade was discovered. When **1** is treated with $NaAlH_4$, with $NaHSO_3$ solution saturated with 0.1 N HCl and finally oxygen (air), **2a** is obtained even though **2b** is the expected product due to the larger number of hydrogen bonds (Scheme 1).[6] The structure of **2a** was characterized by

† Dedicated to Prof. Dr. Peter Köll on the occasion of his 65th birthday.

‡ Universität Konstanz. Fax: ++49-7531-366972.

§ Hans-Knöll-Institut für Naturstoff-Forschung.

|| Carl von Ossietzky Universität Oldenburg.

(1) Gräfe, U. *Biochemie der Antibiotika*; Spektrum Akademischer Verlag: Heidelberg, Germany, 1992.

(2) Priebe, W., Ed. *Anthracycline Antibiotics*; ACS Symposium Series 574; American Chemical Society: Washington, DC, 1995.

(3) Werner, W.; Jütten, P.; Roemer, E.; Haas, W.; Heinisch, L.; Gräfe, U. *Nachr. Chem.* **2000**, *48*, 608.

(4) Ritzau, M.; Vettermann, R.; Fleck, W.; Gutsche, W.; Dornberger, K.-J.; Gräfe, U. *J. Antibiot.* **1997**, *50*, 791.

(5) Oki, T. In *New Approaches for Antifungal Drugs*; Fernandes, P. B., Ed.; Birkhäuser: Boston, 1992.

10.1021/jo0522310 CCC: $33.50
Published on Web 01/10/2006

SCHEME 1. Reaction of Benaphthamycin B (1) To Yield 2a[a]

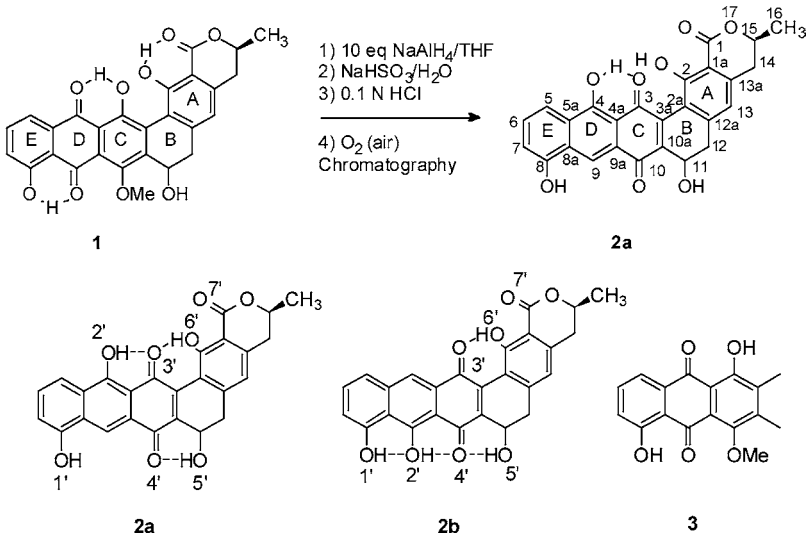

[a] Alternative product **2b** and model compound **3** were used for the theoretical study.

two-dimensional NMR techniques (HMBC, HSQC) and high-resolution (HRES) and electrospray ionization (ESI) mass spectroscopy.[6,7] Finally, the assignment of the absolute configuration of C11−OH and C15−CH_3 was achieved by determination of the X-ray structure of benaphthamycin B (**1**).

The reaction shown in Scheme 1 is a one-pot reaction with a suitable workup, but behind this seemingly simple reaction a complex reaction cascade is hidden, which is still under discussion.[6] Since theoretical investigations significantly contribute to a better understanding of chemical reactions, we report here a computational gas-phase and solvent study to answer two questions: First, can the reaction cascade of the first pathway be supported by calculations? Second, why is the quinone **2a** with the smaller number of hydrogen bonds favored over **2b**? The theoretical analysis of the complete benaphthamycin B reaction sequence is computationally too demanding and will therefore be carried out with a suitable model compound, 1,5-dihydroxy-4-methoxy-2,3-dimethyl-anthraquinone (**3**), which contains all important functional groups.

Computational Details

In the present study all calculations with density functional theory (DFT; employing the hybrid functional B3LYP)[8] and second-order many-body perturbation theory (MP2)[9,10] were performed with Gaussian 03,[11] together with Pople's 6-31G(d)[12] basis set. Transition states were optimized using the Berny algorithm within Gaussian 03. All optimized structures were confirmed as local minima or transition states by calculating harmonic frequencies, and scaled (0.9806) zero-point vibrational energies were obtained. The simulated solvent environment is introduced via Tomasi's polarized continuum model (PCM)[13] using a dielectric constant ϵ of 78.39 (water). Both the perturbation theory and the solvent field data are obtained in single-point calculations employing B3LYP/6-31G(d) geometries. In the following, data from several different levels of theory are given: gas-phase B3LYP/6-31G(d) and MP2/6-31G(d) and solvent (water) B3LYP/6-31G(d) and MP2/6-31G(d), all based on B3LYP/6-31G(d) geometries. For the discussion of the mechanism, only the latter level, PCM-MP2/6-31G(d)//B3LYP/6-31G(d), as the "best" approach is used. The influence of perturbation theory and/or solvation is discussed at the end of the paper.

Results and Discussion

Several theoretical studies on quinones are reported in the literature. AM1 calculations by Lackner[14] predict nonplanar geometries of some of the structures which are bent about the OCCO axis defined by the two quinone carbonyl groups. We have obtained similar results for benzo[*g*]isoquinoline-5,10-dione derivatives.[15] To clarify whether this is a methodical artifact, a search for quinones in the Cambridge Structural Database (CSD)[16] has been performed. It turned out that

(6) (a) Fernekorn, U.; Heinze, T.; Schlegel, B.; Dahse, H. M.; Gräfe, U. *J. Antibiot.* **2001**, *54*, 191. (b) Fernekorn, U.; Heinze, T.; Gräfe, U. Ger. Offen. DE 10043943, 2002.

(7) Fenn, J. B. *Angew. Chem.* **2003**, *115*, 3999.

(8) (a) Becke, A. D. *Phys. Rev. A* **1988**, *38*, 3098. (b) Lee, C.; Yang, W.; Parr, R. G. *Phys Rev. B.* **1988**, *37*, 785. (c) Becke, A. D. *J. Chem. Phys.* **1993**, *98*, 5648.

(9) Møller, C.; Plesset, M. S. *Phys. Rev.* **1934**, *46*, 618.

(10) Head-Gordon, M.; Pople, J. A.; Frisch, M. J. *Chem. Phys. Lett.* **1988**, *153*, 503.

(11) Frisch, M. J.; Trucks, G. W.; Schlegel, H. B.; Scuseria, G. E.; Robb, M. A.; Cheeseman, J. R.; Montgomery, J. A., Jr.; Vreven, T.; Kudin, K. N.; Burant, J. C.; Millam, J. M.; Iyengar, S. S.; Tomasi, J.; Barone, V.; Mennucci, B.; Cossi, M.; Scalmani, G.; Rega, N.; Petersson, G. A.; Nakatsuji, H.; Hada, M.; Ehara, M.; Toyota, K.; Fukuda, R.; Hasegawa, J.; Ishida, M.; Nakajima, T.; Honda, Y.; Kitao, O.; Nakai, H.; Klene, M.; Li, X.; Knox, J. E.; Hratchian, H. P.; Cross, J. B.; Bakken, V.; Adamo, C.; Jaramillo, J.; Gomperts, R.; Stratmann, R. E.; Yazyev, O.; Austin, A. J.; Cammi, R.; Pomelli, C.; Ochterski, J. W.; Ayala, P. Y.; Morokuma, K.; Voth, G. A.; Salvador, P.; Dannenberg, J. J.; Zakrzewski, V. G.; Dapprich, S.; Daniels, A. D.; Strain, M. C.; Farkas, O.; Malick, D. K.; Rabuck, A. D.; Raghavachari, K.; Foresman, J. B.; Ortiz, J. V.; Cui, Q.; Baboul, A. G.; Clifford, S.; Cioslowski, J.; Stefanov, B. B.; Liu, G.; Liashenko, A.; Piskorz, P.; Komaromi, I.; Martin, R. L.; Fox, D. J.; Keith, T.; Al-Laham, M. A.; Peng, C. Y.; Nanayakkara, A.; Challacombe, M.; Gill, P. M. W.; Johnson, B.; Chen, W.; Wong, M. W.; Gonzalez, C.; Pople, J. A., Gaussian, Inc., Pittsburgh, PA, 2004.

(12) (a) Hariharan, P. C.; Pople, J. A. *Theor. Chim. Acta* **1973**, *28*, 213. (b) Pietro, W. J.; Francl, M. M.; Hehre, W. J.; DeFrees, D. J.; Pople, J. A.; Binkley, J. S. *J. Am. Chem. Soc.* **1982**, *104*, 5039.

(13) (a) Miertus, S.; Scrocco, E.; Tomasi, J. *Chem. Phys.* **1981**, *55*, 117. (b) Miertus, S.; Tomasi, J. *Chem. Phys.* **1982**, *65*, 239.

(14) Hoffmann, B. H.; Lackner, H. *Liebigs Ann. Chem.* **1995**, 87.

(15) Opitz, A.; Roemer, E.; Haas, W.; Görls, H.; Werner, W.; Gräfe, U. *Tetrahedron* **2000**, *56*, 5147.

(16) Cambridge Crystallographic Data Centre. http://www.ccdc.cam.ac.uk.

TABLE 1. Hydrogen Bonds Distances (Å) in Products 2a and 2b

bond	2a	bond	2b
O2′H−O3′	1.65	O1′H−O2′	1.78
O5′H−O4′	1.85	O2′H−O4′	1.59
O6′H−O3′	1.65	O5′H−O4′	1.86
		O6′H−O3′	1.63

quinones are usually planar. Even though crystal effects cannot be completely ruled out, it is evident from this analysis that the semiempirical methods cannot correctly reproduce quinone geometries. On the other hand, reliable quinone geometries can be obtained by ab initio methods at Hartree−Fock and DFT levels of theory.[17]

The two alternative products **2a** and **2b** as shown in Scheme 1 differ only in the location of one hydroxyl group that is linked to either C4 or C9 of ring D. Table 1 lists the hydrogen bonds with a distance between the hydrogen atom and the corresponding acceptor atoms equal to or shorter than 1.86 Å. In accordance with the different number of hydrogen bonds in **2a** and **2b**, the experimentally observed compound **2a** is energetically disfavored by 12.6 kcal/mol compared to the alternative product **2b** (B3LYP/6-31G(d)).

On the basis of the experimental data, we propose the following experimental reduction/oxidation pathway for our model system (Scheme 2): In the first step, the reaction starts with the reduction of the quinone carbonyl groups of **3** by $NaAlH_4$, followed by hydrolysis of the aluminum compound. The second step is the formation of the two alternative benzylic carbocations **9a** and **9b** by treatment with 0.1 N HCl and transformation into the anthrones **10a** and **10b**. Here, the cleavage of the phenolic methyl ether takes place to yield anthrones **12a** and **12b**, respectively, which in the last step are oxidized to **13a/b** under formation of hydrogen peroxide. Proof for this sequence, i.e., cleavage before oxidation, is found in the experimental procedure where the reaction mixture is exposed to oxygen as the oxidizing reagent only in the final chromatography.

It is well-known that the phenolic methyl ethers are cleaved under acidic conditions.[15] The reaction mixtures contain not only 0.1 N HCl but also aluminum. We therefore assume that an Al^{3+} species coordinates at the ether oxygen atom, acting as a Lewis acid and thus enabling the S_N2 reaction with water as the nucleophile. In the present study, $Al(OH)_3$ is chosen as a model Lewis acid because of its neutral character; the use of, for instance, $Al(OH_2)_6^{3+}$ would lead to unwanted Coulomb interactions in the gas phase. Subsequently, ion−dipole complexes (**IC1a**, **IC1b**), transition states (**TSa**, **TSb**), and again ion−dipole complexes (**IC2a**, **IC2b**) are formed. The so-called ion−dipole complexes (ICs) were first described by Chandrasekhar[18] for identity S_N2 reactions, then discussed on different levels,[19] and later investigated for nonidentity S_N2 reactions.[20]

An alternative pathway, the 1,3 hydrogen shift in the tetrahydroxy compound **7** and elimination of water with formation of the anthrone **10**, followed by the same steps as described above, can be excluded because it is well-known that 1,3 H shifts are formally forbidden in thermal reactions.

We now want to answer the question of whether the reaction scheme described above can be supported by means of computational studies. The reaction begins with the reduction of **3** by aluminum tetrahydride anion (step 1 in Scheme 2). It proceeds via step-by-step reduction of two quinone oxygen atoms with loss of the quinone system to give two favorable aluminum-containing six-membered rings. Hydrolysis of **6** yields the tetrahydroxy compound **7**. This process is energetically preferential, as shown in Table 2: The formation of **6** relative to the starting compound is favored by 125 kcal/mol; hydrolysis is even more exothermic.

TABLE 2. Relative Energies at Different Levels of Theory (kcal/mol) for Reduction of 3 and Hydrolysis of 6

reaction step	B3LYP/ 6-31G(d), gas phase	B3LYP/ 6-31G(d), solvent	MP2/ 6-31G(d), gas phase	MP2/ 6-31G(d), solvent
3 + $2AlH_4^- + 8H_3O^+ + 4H_2O$	0.0	0.0	0.0	0.0
4 + $2H_2 + 8H_3O^+ + 4H_2O$	−17.9	−34.4	−34.0	−50.5
5 + $2H_2 + 8H_3O^+ + 4H_2O$	−45.2	−63.7	−67.6	−86.8
6 + $2H_2 + 8H_3O^+ + 4H_2O$	−70.9	−92.4	−101.8	−124.8
7 + $2Al(OH_2)_6^{3+} + 6H_2$	−392.4	−470.4	−445.2	−520.7

Protonation of **7** and elimination of water then lead to the carbocations **9a** and **9b**, whose formations are favorable. The stabilization energies of **9a** and **9b** relative to **7** are about 5−10 kcal/mol (Table 3, Figure 1), which can be explained by stabilization of the cationic centers by the adjacent aromatic moieties. Carbocation **9a** is energetically preferred over **9b** by 5.8 kcal/mol. The application of perturbation theory and/or solvent environment does not alter the energetic ordering of the cations; the difference between **9a** and **9b** is always about 5 kcal/mol in favor of the former. Surprisingly, the simulated

TABLE 3. Relative Energies at Different Levels of Theory (kcal/mol) for Ether Cleavage of 7 and Subsequent Oxidation of 12

reaction step	B3LYP/ 6-31G(d), gas phase	B3LYP/ 6-31G(d), solvent	MP2/ 6-31G(d), gas phase	MP2/ 6-31G(d), solvent
7 + $H_3O^+ - H_2O + Al(OH)_3 + O_2$	0.0	0.0	0.0	0.0
8a + $Al(OH)_3 + O_2$	−66.9	−23.6	−56.1	−12.8
8b + $Al(OH)_3 + O_2$	−67.8	−22.6	−57.8	−12.2
9a + $H_2O + Al(OH)_3 + O_2$	−60.9	−22.2	−48.7	−10.3
9b + $H_2O + Al(OH)_3 + O_2$	−55.6	−15.0	−44.8	−4.5
10a + $H_3O^+ + Al(OH)_3 + O_2$	−20.6	−21.8	−14.8	−15.5
10a_enol + $H_3O^+ + Al(OH)_3 + O_2$	−3.7	−9.0	0.9	−4.8
10b + $H_3O^+ + Al(OH)_3 + O_2$	−1.2	−6.7	2.5	−2.7
10b_enol + $H_3O^+ + Al(OH)_3 + O_2$	0.6	−3.4	5.8	1.6
11a + $H_3O^+ + O_2$	−29.7	−27.3	−33.9	−30.2
11b + $H_3O^+ + O_2$	−37.3	−31.8	−37.8	−31.6
IC1a + $H_3O^+ - H_2O + O_2$	−53.9	−41.0	−57.1	−42.3
IC1b + $H_3O^+ - H_2O + O_2$	−41.9	−32.6	−43.0	−53.1
TSa + $H_3O^+ - H_2O + O_2$	−14.4	−4.1	−9.0	2.5
TSb + $H_3O^+ - H_2O + O_2$	−9.3	−1.5	−2.4	6.3
IC2a + $H_3O^+ - H_2O + O_2$	−63.0	−54.5	−61.8	−51.3
IC2b + $H_3O^+ - H_2O + O_2$	−66.2	−54.5	−61.8	−48.9
12a + $H_3O^+ - H_2O + Al(OH)_3 +$ MeOH + O_2	−20.5	−21.4	−10.8	−11.2
12b + $H_3O^+ - H_2O + Al(OH)_3 +$ MeOH + O_2	−15.0	−17.0	−3.7	−5.2
13a + $H_3O^+ - H_2O + Al(OH)_3 +$ MeOH + H_2O_2	−26.2	−36.9	−14.7	−24.9
13b + $H_3O^+ - H_2O + Al(OH)_3 +$ MeOH + H_2O_2	−30.4	−35.5	−17.3	−21.9

(17) (a) Rozeboom, M. D.; Tegmo-Larsson, I.-M.; Houk, K. N. *J. Org. Chem.* **1981**, *46*, 2338. (b) Wheeler, R. A. *J. Am. Chem. Soc.* **1994**, *116*, 11048. (c) Boesch, S. E.; Wheeler, R. A. *J. Phys. Chem.* **1995**, *99*, 8125. (d) Grafton, A. K., Wheeler, R. A. *J. Phys. Chem. A* **1997**, *101*, 7154.

(18) Chandrasekhar, J.; Joergensen, W. L. *J. Am. Chem. Soc.* **1985**, *107*, 2974.

(19) Calculation of nucleophilic substitution: Koch, W.; Holthausen, M. C. *A Chemist's Guide to Density Functional Theory*, 2nd ed.; Wiley-VCH: Weinheim, Germany, 2001; pp 247−249.

(20) (a) Glukhovtsev, M. N.; Pross, A.; Radom, L. *J. Am. Chem. Soc.* **1995**, *117*, 2024. (b) Glukhovtsev, M. N.; Pross, A.; Radom, L. *J. Am. Chem. Soc.* **1996**, *118*, 6273.

SCHEME 2. Proposed Reaction Steps of the Transformation of Model Compound 3[a]

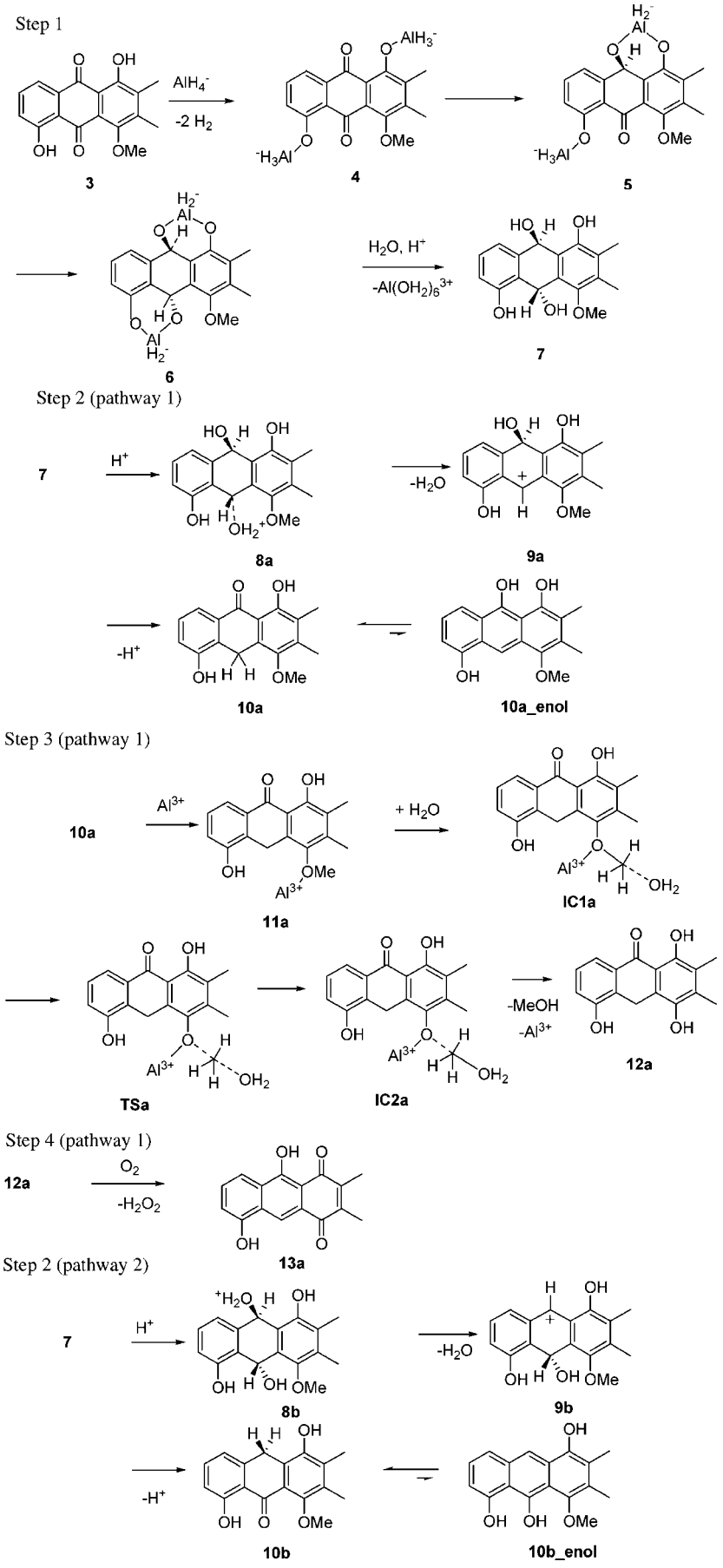

SCHEME 2 (Continued)

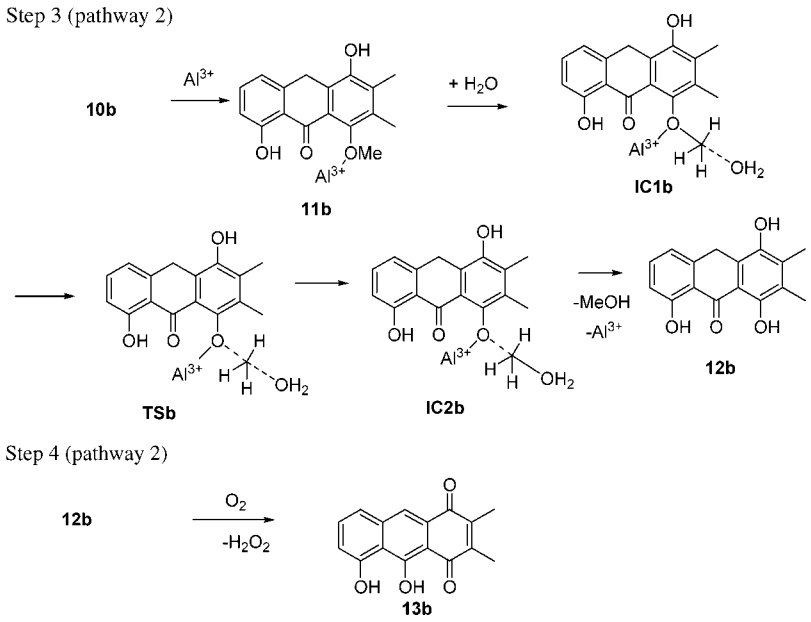

[a] Both alternative pathways leading to products **13a** and **13b**, respectively, are shown.

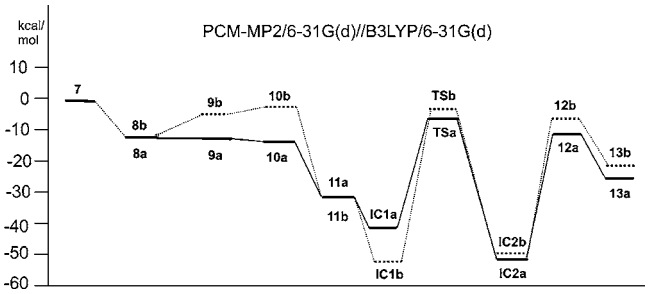

FIGURE 1. Reaction profile for the formation of **13a** and **13b**.

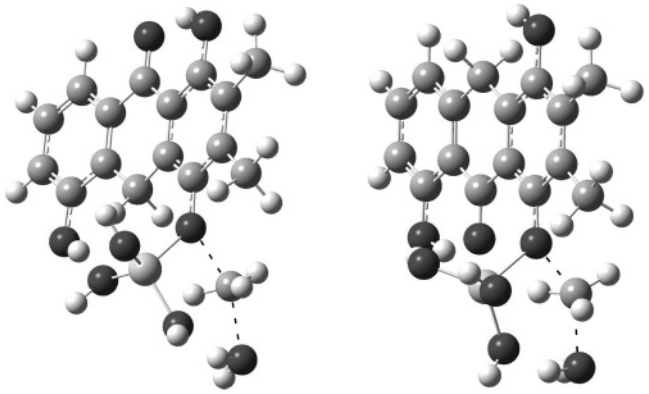

FIGURE 2. Calculated transition states for ether cleavage: **TSa** (left), $d(O-CH_3) = 2.102$ Å and $d(CH_3-OH_2) = 2.007$ Å; **TSb** (right), $d(O-CH_3) = 2.062$ Å and $d(CH_3-OH_2) = 1.996$ Å.

water environment leads to a relative destabilization of the cationic structures **8** and **9** relative to **7**. This might be attributed to the higher stabilization of the hydronium ion in the solvent field compared to the onium ion **8** and the carbocation **9**. The intermediate structures **8** are in fact only loose complexes between the cations and a water molecule with an already broken C−O bond so that the formation of the carbocations **9** cannot be the determining step. The process of simultaneously protonating **7** and breaking the C−O bond to give **8** does not show any activation barrier.

Deprotonation of **9a** (**9b**) leads to the anthrone **10a** (**10b**), whose methyl ether bond is cleaved in the next step of the reaction. In principle, one would expect that the anthroles **10a_enol**/**10b_enol** as tautomeric enol forms should be at least as favorable, but as shown in Table 3 and indicated in Scheme 2, they are significantly less stable and hence should not be formed. An explanation for the stability of the anthrone **10a** (**10b**) might serve the fact that it has two aromatic rings and that there exists a favorable C═O−HO interaction.

We propose on the basis of our calculations and the experimental findings that the ether cleavage proceeds via Lewis acid-assisted nucleophilic attack of a water molecule on the methyl group. We have used $Al(OH)_3$ as a model Lewis acid which coordinates on the phenyl ether oxygen atom (**11a/11b**) and hence activates the O−Me bond. The subsequent S_N2 reaction with water involves two positively charged ion−dipole complexes (**IC1a/b**, **IC2a/b**) and a transition state (**TSa/b**, Figure 2) and leads to the anthrones **12a/b**. The activation energies for these processes also show a slight preference for pathway 1 involving **TSa**, which is favored by 4 kcal/mol.

In the last step of the reaction the quinone is formed. It is well-known that anthroles react with molecular oxygen to give quinone and hydrogen peroxide. This reaction is used in a technical process, the well-known anthraquinone process for the production of hydrogen peroxide.[21] Oxidation of a very similar compound is shown by Koch for tetrahydronaphthacenone.[22] We can therefore safely assume that the oxidation proceeds with formation of hydrogen peroxide. This spin-forbidden oxidation reaction cannot be determined on one reaction coordinate, but the gross reaction energy can be calculated. This reaction is exothermic by about 15 kcal/mol.

(21) Goor, G.; Glenneberg, J.; Jacobi, S. Hydrogen Peroxide. *Ullmann Industrial Chemistry*; Wiley-VCH: Weinheim, Germany, 2002; Vol. A13, p 433.

(22) Schweitzer, B. N.; Koch, T. H. *J. Am. Chem. Soc.* **1993**, *115*, 544.

The data in Table 3 further demonstrate the influence of solvent effects. It is only in the simulated water environment where the transition states become the least stable species of the reaction cascade. This is true for both the B3LYP and MP2 data. The results at these two levels of theory do not differ significantly, with the relative MP2 energies being slightly higher compared to the starting point. The relative destabilization of the positively charges species **8** and **9** has been discussed before.

It is worth mentioning that the reactions steps reduction and hydrolysis, water elimination, and oxidation are exothermic, with the ether cleavage step being thermoneutral, which can be seen as an indication of the accuracy of the proposed reaction mechanism. From our "best" results, we suggest that the complex reaction is kinetically controlled. The difference in activation energies of the S_N2 ether cleavage is decisive for the formed product. Additionally, there is a slight thermodynamical preference for the observed quinone **13a** despite the fewer hydrogen bridges.

Conclusions

The unusual and complex reaction of benaphthamycin B can be explained by theoretical investigations of the reaction with a model compound, 1,5-dihydroxy-4-methoxy-2,3-dimethylanthraquinone (**3**). Calculations of the individual steps (reduction and hydrolysis, water elimination, ether cleavage, and oxidation) of the proposed reaction cascade at the PCM-MP2/6-31G(d)//B3LYP/6-31G(d) level of theory shows that the formation of the thermodynamically preferred quinone **13a** is also the kinetically favored pathway: the ether cleavage as an S_N2 reaction leading to the anthrone **12a** possesses a smaller activation barrier compared to the alternative process yielding **12b**. The results of the calculated model reaction should also be valid for benaphthamycin B (**1**).

Acknowledgment. We gratefully thank Prof. K Diederichs and Dr. J. Sühnel for computation time. This work was supported by additional computer time at the Centre for Scientific Computing at the University Oldenburg.

Supporting Information Available: Table of absolute energies of all calculated level and zero-point vibrational energies and a list of Cartesian coordinates of all calculated structures. This material is available free of charge via the Internet at http://pubs.acs.org.

JO0522310